Captive-Air Irradiation Experiments on Ozone Formation in Southern California

Richard F. Gunst and Nelson A. Kelly*

Abstract

One phase of an air pollution study conducted in the Los Angeles basin during the summer of 1987 consisted of outdoor smog-chamber experiments, called "captive-air irradiation experiments," intended to study the response of ozone to changes in its main precursors, hydrocarbons and oxides of nitrogen. Typically, eight smog chambers (transparent Teflon bags) were filled with ambient morning air at one of the two data-collection sites: downtown Los Angeles or Claremont, a suburb in the eastern part of the Los Angeles basin. One or both of the initial concentrations of hydrocarbon and nitrogen oxides would then be changed in up to seven of the bags by preselected amounts, most of the targeted changes being -50%, -25%, or $+25\%$. Ozone concentrations were measured hourly throughout the day and the maximum of these ozone concentrations in each bag was determined. In this paper, a total of 249 captive-air irradiation experiments conducted on 33 test days are used to obtain empirical models of ozone formation. These fitted models are then used to construct ozone contours as a

* Richard F. Gunst is Professor, Department of Statistical Science, Southern Methodist University, Dallas, TX 75275-0332. Nelson A. Kelly is Staff Research Scientist, Environmental Science Department, General Motors Research Laboratories, Warren, MI 48090-9055. The authors express their appreciation to Gene Fincham and Marty Ruthkosky for assistance with the experimentation, Marty Ferman and Pat Korsog for computational help, and Len Stockberger for making the hydrocarbon measurements.

1

function of the precursor levels, evaluate proposed control strategies intended to reduce ozone levels, and examine the effects of ambient temperature and ultraviolet radiation on the formation of ozone. This is the first time these objectives have been achieved using captive-air irradiation experiments.

An unusual aspect of this environmental study is the use of fractional-factorial experiments to guide the selection of the precursor combinations on approximately one-third of the test days. The remainder of the data consists of more traditional test runs in which the precursor combinations are selected to investigate specific ozone control strategies. Analyses are conducted to assess whether data from the two types of experiments can be combined. An evaluation of the possible effects of bias resulting from the inability to conduct complete factorial experiments on each test day reveals that the effects of the precursor changes on ozone formation are substantially larger than the potential biases. The fractional-factorial portion of the experiment is not only shown to be an improvement over previous design protocols for similar environmental studies, but the major conclusions from analyses of the complete data set are obtainable from analyses of only the smaller fractional-factorial portion of the data.

KEY WORDS: Empirical kinetic modeling; Experimental design; Measurement error

models; Ozone formation; Regression

1. Introduction

In order to devise strategies for reducing ambient ozone concentrations in urban areas, it is necessary to determine the response of the maximum ozone concentrations to changes in their photochemical precursors, nonmethane hydrocarbons (HC) and nitrogen oxides (NO_x). Since the Los Angeles area has the most serious ozone pollution problem in the United States, many scientific studies have been conducted in this region to attempt to understand this relationship. One of the most ambitious studies undertaken in this region is the Southern California Air Quality Study (SCAQS) conducted during the summer of 1987.

2

As part of this comprehensive study, experiments were conducted to measure the response of ozone to precursor changes by trapping morning ambient Los Angeles air in the outdoor smog chambers (transparent Teflon bags), altering the HC and NO_x in some of the chambers, and measuring the ozone that was subsequently formed (Kelly and Gunst 1989). Such experiments have been termed "captive-air irradiation" (CAI) experiments.

CAI experiments simulate initial conditions in the polluted atmosphere, and the changes in the initial HC and NO_x represent possible pollution control strategies. Such experiments have proven useful in simplifying complex atmospheric conditions, allowing the testing of just the chemical portion of the atmospheric system (Kelly 1985, 1988). Furthermore, the CAI experiments, which use sunlight and actual pollutants in multiple chambers, are a special type of smog chamber experiment that are closer to real atmospheric conditions than traditional laboratory studies that use artificial light and a simple HC-NO_x mixture in a single chamber (Dunker 1988).

The investigations reported in this paper detail major advances in the design of CAI experiments and in the modeling of ozone concentrations that were achieved in the 1987 SCAQS experiments. In particular, this paper shows that the design used systematically interrogates the experimental region of interest; moreover, the fractional-factorial portion of the experiment, using approximately one-third of the experiments, would have sufficed to adequately model the ozone concentrations. Polynomial reponse surface models are fit to the ozone concentrations. Ozone contours derived from the fitted polynomial models enable an evaluation of three pollutant control strategies for reducing ozone: (a) reducing both pollutants equally, (b) reduce only HC, and (c) reduce only NO_x.

Key features of the CAI experimentation are summarized in Section 2. Statistical considerations used to guide the experimentation are detailed in Section 3. Characteristics of the data base, initial least squares model fits, and a discussion of the techniques used to verify the reasonableness of model assumptions are described in Section 4. A (nonlinear) polynomial measurement error model is fit to the data in Section 5. Contour plots derived from the fitted model are then used to evaluate the three

proposed ozone control strategies. Concluding remarks about the fractional-factorial portion of the experiment are made in Section 6.

2. CAPTIVE-AIR IRRADIATION EXPERIMENTS

Captive-air irradiation experiments (see Figure 1) consist of filling 500 liter pillow-shaped transparent Teflon bags (smog chambers) with morning ambient air, increasing (spiking) or decreasing (diluting with "clean air", air that contains negligible amounts of HC and NO_X) the ambient concentrations of HC and/or NO_X by prespecified amounts, and measuring the concentrations of ozone in each bag hourly throughout the day. Although nine bags were potentially available each day of the SCAQS study, one of the bags was reserved for chemical analyses that required large volumes of air, so only eight could be used to determine ozone formation. For example, the HC measurements used in the modeling of the maximum ozone concentrations were provided by the Environmental Protection Agency from gas chromotography (g.c.) measurements on air samples furnished from the ninth bag.

All nine bags were initially filled with morning ambient air. At least one of the eight test bags on each day was not altered. The unaltered bags are used as control bags against which ozone measurements in the altered bags can be compared. The need for control bags on each test day is well illustrated by Figure 2. This figure shows the distribution of initial HC (ppbC) and NO_X (ppb) concentrations in the 47 of the 62 control bags for which data are available on both of the precursors. The wide distribution reflects the daily differences in ambient concentrations of the precursors, differences which affect the amount of ozone formed. Had the control bags not been included, the effects due to changes in the precursors specified by the experimental design would have been confounded with effects due to different initial ambient concentrations.

A detailed explanation of spiking and dilution procedures is provided in Kelly and Gunst (1989). The basics of the procedures are as follows. When the control bag was approximately 80% filled with morning ambient air, the amount of NO_X in the control bag was measured. Nonmethane hydrocarbon measurements were determined by g.c., the results of which were not immediately available. For

4

spiking and dilution purposes, the amount of HC in the morning ambient air was estimated from the initial NO_x measurement in the control bag and the typical ratio of HC to NO_x for the Los Angeles basin, $HC/NO_x = 10$. If a bag simply required increasing HC or NO_x, the required additions were made during the final stages of filling with ambient air. Bags which required reductions in one or both of the precursors were first filled with ambient air, then partially evacuated, typically by 25% or 50% of their volumes. A mixture of clean air and known amounts of the precursors was then added to achieve the desired change from ambient concentrations. For example, if a bag required a reduction of 25% in HC and no change in NO_x:

(a)   25% of the ambient air was evacuated,

(b)   an amount equivalent to the 25% of the initial NO_x that was removed during the

evacuation was then added back to the bag as it was filled with clean

air from a pressurized cylinder.

Initial ozone measurements in morning ambient air were very low; consequently, the dilution process mentioned above can be regarded as having no effect on the amount of ozone initially present in the bags. Both ozone and NO_x measurements were taken hourly throughout the day in each of the eight bags. The maximum ozone concentration (ppb) for each bag was obtained from the hourly measurements, typically the 5:00 p.m. measurement.

3. EXPERIMENTAL DESIGN

Two sites in Southern California were used for the CAI experiments. The downtown Los Angeles site was chosen because it is an urban location near large precursor emissions sources. Claremont, a surburban location approximately 45 km east of downtown Los Angeles, was chosen because it is further removed from major emissions sources and is a downwind ozone receptor site.

CAI experiments were conducted on 17 days between June 12 and July 7 in downtown Los Angeles. At the Claremont site, CAI experiments were conducted on eight days between July 12 and July 27 and on eight days between August 19 and August 28. Unfavorable weather in July caused the

break in experimentation at the Claremont site. A total of 249 CAI experiments were conducted over the 33 test days.

The Environmental Protection Agency utilizes a chemical kinetic model, known as the empirical kinetic modeling approach (EKMA), to predict maximum ozone concentrations as a function of initial HC and NO_x. Theoretical ozone contours (isopleths) from this model suggested that 25% and 50% reductions in the ambient precursor concentrations and a 25% increase in the ambient concentrations would permit a satisfactory interrogation of the effects of precursor changes on ozone formation in the Los Angeles basin, based again on a typical HC/NO_x ratio of 10 for the area (Kelly and Gunst 1989). Precursor reductions were emphasized in planning the CAI experiments in order to allow investigation of ozone control strategies. The expected changes in ozone were sufficiently large that a 10% anticipated experimental error would not mask the expected effects due to changes in the precursors.

Six test days were allocated for the statistically designed portion of the CAI experiments at each location. This portion of the experimental design was specifically included to permit the modeling of ozone as a function of the initial precursor concentrations. The additional 21 test days were devoted to investigations of specific ozone control strategies and other experiments that were not part of the statistical design, although some were very similar to those in the statistical design. Approximately half of the 33 test days contained replicate tests, in which two or more bags were filled with identically prepared mixtures. These replicate measurements were included in the experiment to ensure quality control in the measurement process, to allow the estimation of uncontrolled experimental variability, and to gauge the feasibility of including test results from both portions of the experiment in one data base for analysis.

The four precursor levels included in the experimental design were -50%, -25%, 0, and +25%, where 0 refers to the initial ambient concentration in morning air and the other three levels indicate percentage changes from the initial ambient concentration. Since only eight test bags were available, complete factorial experiments in the four levels of each of the precursors could not be conducted on any test day. Consequently, a half fraction of a complete factorial experiment was conducted on each

6

of four of the six days at each location. The half fraction selected on each day was selected according to the procedure outlined in the appendix, and always included a control bag. Quarter-fractions, with each of three precursor combinations and a control replicated in two of the eight test bags, were run on the remaining two of the six test days at each site.

As with all fractional-factorial experiments, the question of confounding of effects is of concern. By confounding different effects on each day, it was hoped that the partial confounding patterns that resulted would tend to ameliorate the possible biases. Statistical support that this occurred for the entire set of test runs, including the special-purpose test runs for which the confounding pattern is unknown, is given in the next section.

Figure 3 displays the target precursor levels, expressed as a percentage change from ambient concentrations, for the six-day fractional-factorial portion of the experiment at each location. The plotting symbol identifies the test day on which each of the combinations occurred. The selected combinations include all factor-level combinations at least once. Observe that the control bag is included on each test day, twice on two of the test days. The combination RHC $= RNO_x = -25\%$, where "R" denotes a relative change of -25% from initial ambient concentrations, appears six times in the experiment. Some consideration was given to modifying the design so that one or two of these test bags could be used for other combinations; however, it was decided to use the design as shown because the combination RHC $= RNO_x = -25\%$ is an important combination of interest in proposed control strategies for ozone reduction. Prior to executing the experimental design the assignment of the precursor combinations to the individual smog chambers was randomized.

Because of measurement errors and differences in the initial ambient amounts of NO_x in the control bag(s) and in the other test bags on a given day, the achieved precursor changes in the individual bags differ from the target values. The differences between the actual (percentage) changes and the target (percentage) changes averaged 30% of the target values for HC and 21% for NO_x.

Figure 4 is a scatterplot of the initial HC and NO_x concentrations obtained in the study, by site. The NO_x concentrations are the initial ambient measurements obtained from each of the eight bags on

each test day. The initial HC measurement for a particular bag is calculated from the HC measurement provided by EPA from the ninth bag on each test day, the initial NO_x measurement taken from the control bag for that day, the initial NO_x measurement for that particular bag, and any added HC (see Kelly and Gunst 1989, Appendix A). Comparison of Figures 2 and 4 shows that the experimental design, including both the fractional-factorial and the special experiments, expanded the experimental region well beyond the ambient levels of HC and NO_x observed in the control bags.

4. INITIAL MODEL FITS

Of the 249 observations in the data base, 234 contained measurements on all the variates of interest in this experiment. In the complete (n=234) data set, 94 of the observations are from the portion of the experiment stipulated by the fractional factorials described in the appendix. The remaining 140 observations form the special-purpose spiking and dilution experiments. One of the questions first examined was whether the two portions of the complete data could be combined into one data base for preliminary least squares fitting of the maximum ozone concentrations.

To answer this question, linear model analyses of the effects of the changes in the precursors on ozone formation for the two types of experiments were performed. The maximum ozone concentrations were modeled as a function of main effects for the type of precursor change from ambient levels and for the type of experiment, and the interaction between these two factors. The interaction was included as the primary indicator of possible differential effects of the precursor changes for the two types of experiments. While the main effect for the type of experiment was found to be statistically significant ($p = .01$), the interaction variable was not ($p = .18$). A comparison of the variance estimates from the replicate test runs also revealed no statistically significant differences between the two sets of experiments. Based on these analyses, the fractional-factorial and the special-purpose test runs were combined into one data base for least squares model fitting.

In conjunction with the foregoing analyses and the polynomial model fitting described below, the assumption of normally distributed errors was examined. Residual plots, statistical tests for normality,

8

and Box-Cox power transformations were used to confirm the reasonableness of this assumption. For example, the 95% confidence interval on the transformation parameter of the single-parameter Box-Cox power transformation (Box and Cox 1964) is $.75 \leq \lambda \leq 1.10$, with the maximum likelihood estimate $\hat{\lambda}$ = .95. Although one might expect the maximum ozone concentrations to follow an extreme value distribution, the normal distribution is a reasonable assumption since most of the maxima occurred at 5:00 p.m.; i.e., the maximum ozone concentrations behave like a sample of 5:00 p.m. ozone measurements rather than a sample of maximum order statistics. Investigation of other traditional model assumptions (e.g., homoscedasticity) during the course of the model fitting process led to the conclusion that these assumptions were also reasonable for the CAI data base.

A few influential observations were discovered. These outliers occur because the fitted models examined were unable to satisfactorily fit ozone concentrations for a small number of the most extreme precursor changes: large reductions of HC accompanied by either no change or an increase in NO_x. The three largest studentized residuals were associated with the precursor combinations HC = -50%, NO_x = +25%. The influential observations did not substantively affect the estimated regression coefficents in the final models or the inferences that were subsequently drawn; consequently, they were retained in the data base.

A key concern during the design phase of the experiment was the possible confounding effects of day-to-day variability of ambient ozone and ambient precursor levels with the effects of the precursor changes. Since complete factorial experiments could not be conducted on each day of the study, day-to-day variability of the initial precursor concentrations could bias any observed effects of the designed precursor changes. Figure 2 confirms the existence of this large day-to-day variability.

Figure 5 is a box plot, (e.g., Mason, Gunst, and Hess 1989, Section 4.3) of the precursor effects, with a separate box for each of the nine precursor combinations that occurred most frequently in the experiment. The precursor changes are shown in parentheses above each box; e.g., (0, -25) represents RHC = 0, RNO_x = -25%. The effects plotted are the differences between the maximum ozone concentration for a test bag on a given day and the maximum (average) ozone concentration for the

9

control bag(s) on the same day. Each box contains the responses for all the days that have one type of precursor change. The five-number summaries (minimum, lower quartile, median, upper quartile, maximum) in each box plot thus portray the day to-day variability of the effects of a specific (HC, NO_x) change from ambient levels. The number beneath each box indicates the number of ozone differences in the data set for that HC-NO_x change.

Two characteristics of these plots are pertinent to the concern over day-to-day biases. First, most of the boxes are centered well away from zero, indicating strong effects of the precursor changes. Second, the variability in the boxes does not extend over a wide enough range to mask the strong precursor effects. Some of the boxes do not overlap; others have only minor overlap. Together, these findings indicate that, while biases due to day-to-day differences may exist, the precursor effects are sufficiently strong to enable an adequate assessment of their influence on the formation of ozone. In the next section, comparison of fitted ozone contours with those of the EKMA mechanistic modeling approach provides further support for this conclusion.

Use of four target concentration levels of each precursor would allow up to a third-degree polynomial to be fit to the ozone concentrations. As a design consideration, this was believed to be sufficient to adequately model the expected nonlinear dependence of the ozone concentrations on the HC and NO_x mixtures, as suggested by the EKMA ozone contours. Since the actual precursor concentrations differed from the target values, the actual values rather than the target values were used in all regression models. Initial regression fits indicated that positive powers of the precursor concentrations would not sufficiently capture the nonlinear nature of the relationship.

An investigation of polynomial terms of the form $NO_x{}^a/HC^b$ greatly improved the fit over quadratic and cubic polynomials. An adequate number of ozone replicates (68 degrees of freedom) were available to test for model lack of fit. Substantial lack of fit was observed in all models that involved only the precursors. Four covariates were available for possible inclusion in the model: average and maximum hourly ambient temperature, and average and maximum measures of ultraviolet radiation. Special tests using only clean air spiked with an a known amount of the precursors demonstrated a

10

strong temperature effect on the formation of ozone. When added to the regression models, the average daily temperatures contributed substantially to reducing the lack of fit in all the better models investigated. The measures of ultraviolet radiation, which varied by approximately $\pm$ 15% from the average value for the data set, did not contribute substantively to improving the fits.

Reformulating the model with alternative response variables does not eliminate the lack of fit. The difference in ozone concentrations between each bag and the (average) ozone concentration for the control bag(s) on the same day, as well as the ratio of these two variates, was examined. Alternative response variables were ultimately discarded not only because they failed to eliminate the lack of fit, but also because their use would impair the investigation of control strategies that are intended to reduce the actual concentrations of ozone.

The final model selected consists of three terms: NO_x (N), average ambient temperature (T), and the ratio NO_x^2/HC (Q). This is the best fitting three-term model from candidate models involving polynomial terms NO_x^a/HC^b with a, b = $\pm$ .5, $\pm$ 1, $\pm$ 2, and $\pm$ 3. No fits examined that involved four or more polynomial terms substantially altered the characterization of the ozone concentrations in contour plots. Additional indicator variables for site (LA vs. Claremont) and type of experimental design (fractional-factorial vs. special purpose) were not statistically significant. There are alternative fits that compete with this three-term fit on the basis of model summary statistics such as C_p, but these alternative fits involve more complicated polynomial functions of NO_x and HC, and the additional polynomial terms generally induce strong collinearities. The three-term least squares fit, with estimated standard errors in parentheses is:

$$Ozone = -280.7 + 2.8N - 6.4Q + 19.4T \ . \tag{4.1}$$

$$(26.8) \quad (.1) \quad (.4) \quad (1.3)$$

5. MEASUREMENT ERROR MODEL FITS

The two precursors, HC and NO_x, are subject to a variety of uncontrollable measurement errors. Not only is there error due to the measurement process itself, error is also introduced because of the

11

inability to exactly duplicate initial morning ambient levels in the control and in the test bags and to exactly hit the targeted changes in the precursor values. The least squares analyses reported in the last section were conducted to identify a tentative model for fitting ozone contours and to initially assess the adequacy of several model assumptions. In this section the three-term ozone model is fit under the more realistic assumptions of measurement error models.

A nonlinear measurement error model is fit to the data in order to account for the measurement errors in the estimation of the regression coefficients. The measurement error model is nonlinear because the ratio Q is nonlinear in the true (error-free) precursor values. The model in implicit form is $f(\xi, \beta) = 0$, where

$$f(\xi, \beta) = \psi - \beta_4\pi_4 - \beta_1\pi_2 - \beta_2\pi_2^2/\pi_1 - \beta_3\pi_3 . \qquad (5.1)$$

In this model, $\xi = (\psi, \pi')'$ represents the true unobservable response and predictor variables, with maximum daily ozone represented by ψ and the predictors represented by π_1 (HC), π_2 (NO$_x$), π_3 (TEMP), and the constant term by $\pi_4 = 1$.

The measurable variates are $z = (y, x')' = \xi + w$, where w is a vector of measurement errors. The analyses performed with these data assume that the true predictors represent unknown constants (functional model) and that the errors are mutually independent with $w_i = (v_i, u_i')' \sim N(0, \Sigma_{ww})$ and $\Sigma_{ww} = diag(\sigma_{vv}, \Sigma_{uu})$, where

$$\Sigma_{uu} = \begin{bmatrix} \sigma_{11} & \sigma_{12} & 0 & 0 \\ \sigma_{12} & \sigma_{22} & 0 & 0 \\ 0 & 0 & 0 & 0 \\ 0 & 0 & 0 & 0 \end{bmatrix} .$$

The zeros in the last two rows and columns indicate the temperature variable ($x_3 = \pi_3$) and the constant term ($x_4 = \pi_4 = 1$) are considered error-free (temperature variability is considered below).

12

From the replicates in the data base, the ozone error variance and the HC and NO_x error variances and covariance can be estimated. The estimates, based on 55 degrees of freedom, are:

$$\hat{\sigma}_{vv} = 79 \qquad \hat{\sigma}_{11} = 265 \qquad \hat{\sigma}_{22} = 6 \qquad \hat{\sigma}_{12} = 34 \quad .$$

The vector of averages $\bar{z}$ and the sample covariance matrix, $S_{zz} = (n\text{-}1)^{-1} \sum (z_i - \bar{z})(z_i - \bar{z})'$, of the observed ozone and precursor variates, calculated from the $n = 234$ observations with complete data, are:

	Ozone	HC	NO_x	TEMP	
$\bar{z} = ($	269	631	78	21	$)'$

$$S_{zz} = \begin{bmatrix} 7{,}588 & 19{,}475 & 2{,}419 & 93 \\ & 92{,}934 & 6{,}005 & 191 \\ & & 1{,}408 & 20 \\ \text{sym} & & & 3 \end{bmatrix}$$

Comparison of the magnitudes of the estimated error variances $\hat{\sigma}_{vv}$, $\hat{\sigma}_{11}$, and $\hat{\sigma}_{22}$ with the corresponding sample variances in S_{zz} reveals that the magnitudes of the estimated error variances are less than 2% of those of the corresponding sample variances of the observed variates.

The nonlinear measurement error model (5.1) was fit using an adaptation of the Gauss-Newton iteration scheme of Fuller (1987, Section 3.3.2). The 179 averages over replicates for the complete data (n=234) were used in the fitting procedure, a weighted version of Fuller's equation (3.3.17) derived by minimizing his equation (3.3.19) with the error covariance matrix Σ_{uu} replaced by $r_i^{-1}\Sigma_{uu}$ in the iteration scheme to accommodate the unequal replication (r_i) in the averages. Standard errors were estimated using Fuller's asymptotic covariance matrix (3.2.20). The fitted model, with estimated standard errors in parentheses, is:

$$\text{Ozone} = -280.2 + 2.8N - 6.5Q + 19.3T \ . \tag{5.2}$$
$$(26.4) \quad (.1) \quad (.4) \quad (1.3)$$

This fit is virtually identical with the least squares fit, equation (4.1), due to the relatively small error variances. Several additional analyses were conducted in order to assess the sensitivity of the measurement error model fit to the assumptions about the error variances. One additional analysis that was conducted examined the error-free assumption for the average hourly temperatures. In practice temperature is not measured error free. A small amount of data ($n = 58$) was available from two thermocouples that measured temperature every five minutes over a four-hour period. These data were used to estimate the temperature error variance, assuming uncorrelated errors and equal error variances for the two thermocouples. The average temperatures in the data sets were based on 15 hourly readings each day. From this information, the estimated error standard deviation for the average temperatures is .02 °C.

A second analysis examined the assumption of correlated HC and NO_x errors. While the replicate data provide a nonzero covariance estimate for the HC and NO_x errors, a theoretical argument can be made that the errors should be uncorrelated. Neither of these two, nor any of the other additional analyses that were conducted, resulted in substantive changes in the fitted model. The estimated regression coefficients changed by no more than two units in the third significant digit.

Figure 6 is a contour plot of the fitted ozone concentrations, equation (5.2), for an average ambient temperature of $T = 21.1°C$. The contours are not elliptical. There is a noticeable bending for high NO_x and moderate to low HC values. These contours are qualititatively similar to those derived from the EKMA modeling approach. This fit constitutes the first solely empirical corroboration of the shape of the EKMA contours for the Los Angeles basin.

The contours show two rate limiting regions. A "NO_x-inhibition region," in which decreases in NO_x result in higher concentrations of ozone, occurs at low HC/NO_x. A "HC-saturation region", in which decreases in HC have no appreciable effect on ozone concentration, occurs at high HC/NO_x.

14

Between these regions is a ridge, the "knee region," along the fitted ozone surface where the ozone concentration changes with both HC and NO_X. These regions are clearly seen in the view of the fitted ozone surface shown in Figure 7.

The fitted contours can be used to evaluate the three possible ozone control strategies: (a) reduce both pollutants equally, (b) reduce HC only, or (c) reduce NO_X only. If the HC/NO_X ratio is low, strategy (b) is most effective for the large ozone reductions needed in the Los Angeles basin because of the NO_X-inhibition region of the contour plot. If the HC/NO_X ratio is high, strategy (c) is effective because of the HC-saturation region of the contour plot. Strategy (a) does not appear to be as effective as either of the other two, even if the HC/NO_X ratio is moderate, because of the distance between contours along the "knee" of the plot. This could partially account for the limited success in recent years with this control strategy in Los Angeles. The ambient morning HC/NO_X average in this data set is $631/78 = 8$. This ratio defines a line slightly above the center of the knee region in Figure 6, suggesting that strategy (b) may be preferable to (a) for the Los Angeles basin. From Figure 2, it appears that the Los Angeles basin was typically in the knee region during the summer of 1987.

6. THE FRACTIONAL FACTORIAL EXPERIMENTS

The design and execution of this experiment culminate in important contributions to the evaluation of relationships between ozone and its precursors for the Los Angeles basin through modeling of the ozone as a function of HC, NO_X, and average daily temperatures. During initial planning of the experiment, consideration was given to two important objectives: the need for explicit evaluation of control strategies on individual test days, and the statistical requirements for modeling ozone as a function of the primary pollutants, nonmethane hydrocarbons and oxides of nitrogen. These two considerations led to the design of the special-purpose experiments and to the fractional-factorial experiments, respectively. Ultimately, both types of experiments were able to be combined into one data base for analysis.

The fractional-factorial portion of the experiment has important consequences for the design of

15

similar experimental studies in the future. Figure 8 shows the distribution of the observed precursor combinations for the fractional-factorial and the special-purpose test runs. Note that the fractional-factorial portion of the experiment interrogates the experimental region as well as the special test runs and appears to be more uniformly dispersed.

Location and scale differences exist between the two portions of the experiment:

	Special Test Runs		Fractional Factorials	
	HC (ppbC)	NO_x (ppb)	HC (ppbC)	NO_x (ppb)
Average	509	67	814	93
Standard Deviation:	215	32	328	40

The location and dispersion differences are due to the intended selection of many of the special-purpose test runs to investigate pollutant reduction strategies, thereby resulting in lower pollution targets and reduced variability compared to the fractional-factorial portion of the experiment.

The measurement error model coefficient estimates for the two portions of this data set are:

$$Ozone = -377.9 + 2.8N - 6.9Q + 24.2T \qquad \text{(fractional factorial)}$$
$$(66.9) \quad (.2) \quad (.6) \quad (3.4)$$

and

$$Ozone = -258.7 + 2.6N - 5.4Q + 18.3T \qquad \text{(special test runs)}$$
$$(24.2) \quad (.1) \quad (.6) \quad (1.2) \qquad .$$

Accounting for the location and scale differences for the two portions of the data set, the coefficient

estimates from the fractional-factorial data are remarkably close to those from the complete data set for both the least squares and the measurement error model fits. Other analyses of the fractional-factorial portion of the data set are also similar to those of the complete data set. For example, the three-variable polynomial selected as the best of the three-variable candidate models for least squares fits to the complete data set in the last section is also identified as one of the two best three-variable subsets for the least squares fits to the fractional-factorial experiment, the other one including the three terms NO_x^2, NO_x^3/HC, and average ambient temperature. The fitted ozone contours using only the fractional-factorial portion of the data set are very similar to those for the complete data set.

All of these similarities between the results for the fractional-factorial experiment and the complete data set occur precisely because the fractional factorial adequately interrogates the HC-NO_x region of interest through the careful selection of the HC-NO_x combinations, resulting in the distribution shown in Figure 8. Prior to the execution of the experiment, it was unknown whether the special-purpose test runs, some of which were selected as the experiment progressed, would enable a comprehensive investigation of statistical issues related to the modeling of ozone formation. The fractional-factorial experiment provided such assurances and could have been used to model the ozone formation even if the two data sets could not be combined. Of equal importance to its contributions to the fitting of ozone contours in this data set is the implication for future air pollution studies of this type: careful statistical planning of the experimental test sequence can result in comprehensive analyses and model fits with economically efficient experimental designs.

APPENDIX: SELECTION OF FRACTIONAL FACTORIAL TEST RUNS

Half fractions of the 16 combinations of levels for HC and NO_x were obtained by the following procedure (e.g., Mason, Gunst, and Hess 1989, Chapter 9).

1.   Recode each factor as two two-level factors; e.g., recode the four levels of HC as levels of two factors HC_A and HC_B:

Original HC Levels: -50 -25 0   25

17

Recoded HC_A Levels: -1 -1 1 1

Recoded HC_B Levels: -1 -1 -1 1 .

2. Write the three single-degree-of-freedom main effect contrasts for each original factor in terms of the recoded factors; e.g., $HC_1 = HC_A$, $HC_2 = HC_B$, and $HC_3 = HC_A x HC_B$:

Combination	HC_1	HC_2	HC_3	NO_{X1}	NO_{X2}	NO_{X3}
1	-1	-1	1	-1	-1	1
2	-1	-1	1	-1	1	-1
3	-1	-1	1	1	-1	-1
4	-1	-1	1	1	1	1
5	-1	1	-1	-1	-1	1
$\vdots$						
16	1	1	1	1	1	1 .

3. Determine the nine interaction single-degree of freedom contrasts for the original factors from the products of the main effect contrasts for the recoded factors; i.e., $(HCxNO_X)_1 = HC_1 x NO_{X1}$, $(HCxNO_X)_2 = HC_1 x NO_{X2}, \ldots, (HCxNO_X)_9 = HC_3 x NO_{X3}$,

4. For a half fraction of the original 16 combinations, select one of the interaction contrasts. Run the eight test runs whose signs are the same as that of the control bag $RHC = RNO_X = 0$. Use a different contrast for each of the four test days on which half-fraction is to be conducted.

5. If a quarter fraction is to be run, select two interaction contrasts and the four test runs that have the same signs as the control bag on both of the two interactions. Use different interactions for the two test days on which a quarter fraction is to be conducted.

18

REFERENCES

Amemiya, Y. and Fuller, W. A. (1988), "Estimation for the Nonlinear Functional Relationship," *The Annals of Statistics*, 16, 147-160.

Box, G.E.P. and Cox, D.R. (1964), "An Analysis of Transformations," *Journal of the Royal Statistical Society, Series B*, 26, 211-246.

Britt, H.I. and Luecke, R.H. (1973) "The Estimation of Parameters in Nonlinear Implicit Models," *Technometrics*, 15, 233-247.

Dunker, A.M. (1988), "Uncertainty Analysis and Captive-Air Studies as Aides in Evaluating Chemical Mechanisms for Air Quality Models," Research Publication No. GMR-5844, General Motors Research Laboratories, Warren, MI

Fuller, W.A. (1987), *Measurement Error Models*, New York: John Wiley.

Kelly, N.A. (1985), "Ozone/Precursor Relationships in the Metropolitan Detroit Area Derived from Captive-Air Irradiations and an Empirical Photochemical Model," *Journal of the Air Pollution Control Association*, 34, 27-34.

Kelly, N.A. (1988), "Photochemical Ozone Formation in Outdoor Smog Chambers and Its Sensitivity to Changes in Precursors at a Surburban Detroit Site," in Wolff, G.T., Hanish, J.L., and Schere, K.L. (eds.), *The Scientific and Technical Issues Facing Post* 1987 *Ozone Control Stratigies*, Pittsburgh, PA: The Air Pollution Control Association.

Kelly, N.A. and Gunst, R.F. (1989), "Response of Ozone to Changes in Hydrocarbons and Nitrogen Oxides Concentrations in Outdoor Smog Chambers Filled with Los Angeles Air," Research Publication GMR-6668, General Motors Research Laboratories, Warren, MI.

Mason, R.L. , Gunst, R.F. , and Hess, J.L. (1989), *Statistical Design and Analysis of Experiments*, New York: John Wiley.

Wolter, K. M. and Fuller, W. A. (1982). "Estimation of Nonlinear Errors-in-Variables Models," *The Annals of Statistics*, 10, 539-548.

19

FIGURE TITLES

Figure 1.   Instrumentation and Smog Chambers for Captive-Air Irradiation Experiments.

Figure 2.   Nonmethane Hydrocarbon and Nitrogen Oxides Combinations in Control (Ambient Air) Bags.

Figure 3.   Target Relative Changes (%) in Precursor Values, from Ambient Levels.
The symbols plotted in each cell indicate the test days on which the combination (RHC, RNO_x) for that cell is to be tested.

Figure 4.   Distribution of Realized Precursor Combinations Throughout the Experimental Region. These are the actual precursor values in the test bags following any dilution or spiking.

Figure 5.   Box Plots of Day-to-Day Variability in Ozone Differences from Control Bags. Each box is a five-number summary (minimum, lower quartile, median, upper quartile, maximum) of the maximum ozone concentrations for all days with the (RHC, RNO_x) percentage changes indicated over the respective boxes.

Figure 6.   Fitted Ozone Contours: Nonlinear Measurement Error Model Fit.

Figure 7.   Fitted Ozone Surface: Nonlinear Measurement Error Model Fit.

Figure 8.   Distribution of Realized HC and NO_x Combinations.
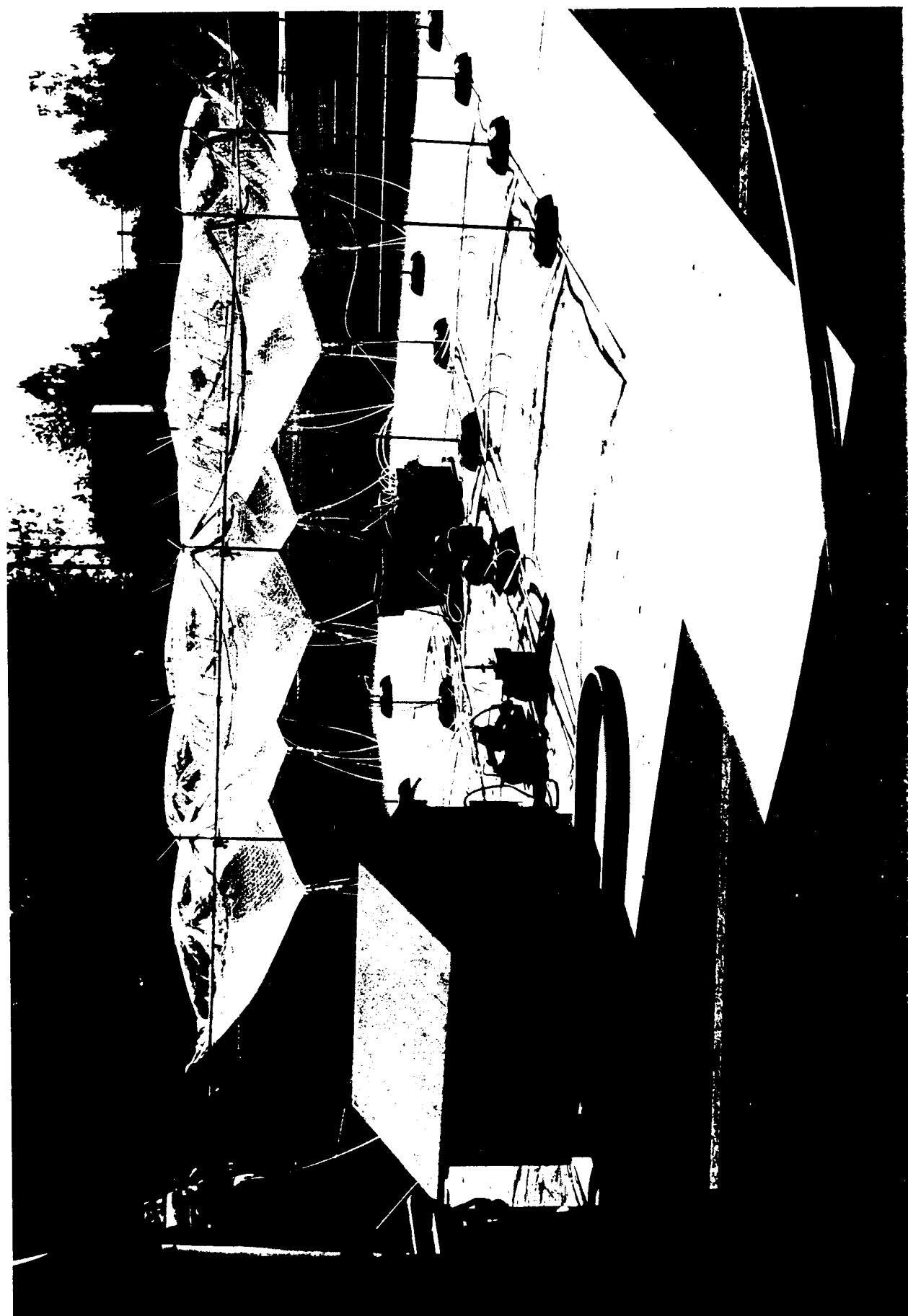
Fig. 2. Hydrocarbon and Nitrogen Oxides Combinations
In Control (Ambient Air) Bags

● = DOWNTOWN LOS ANGELES

○ = CLAREMONT

NOx (ppb)

HC (ppbC)
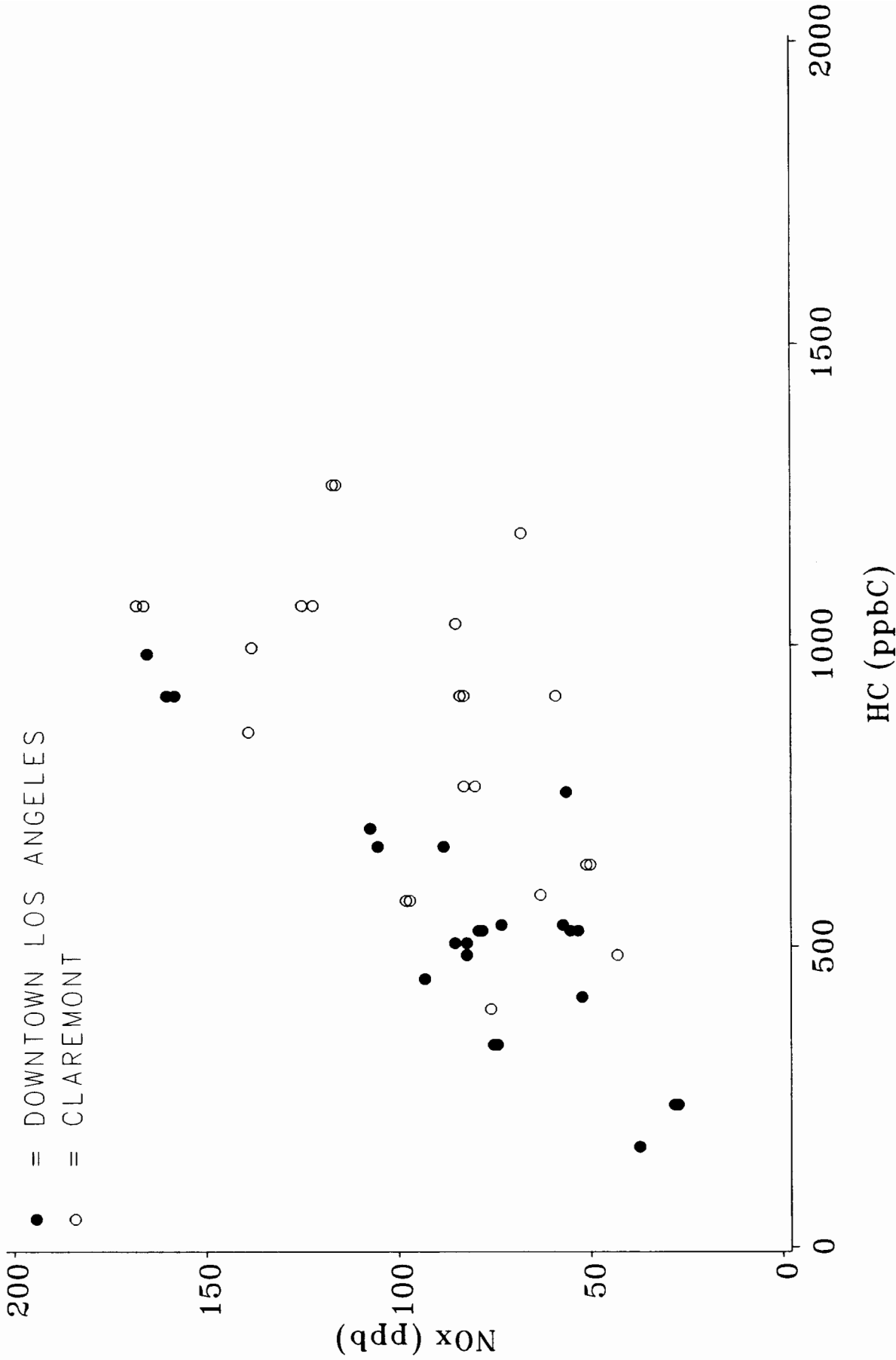
Fig. 3. Target Percentage Changes in Precursor Values, From Ambient Levels
(Plotting Symbol is the Test Day)

Relative Change in NOx	Relative Change in HC: −50	−25	0	25
25	2 3 4	3 1	2 5 5	1 4 5 5
0	1 2	4 6 6	1 2 3 4 / 5 5 6 6	3 5 5
−25	3	1 2 3 / 4 6 6	4 6 6	1 2
−50	1 4	2	1 3	2 3 4
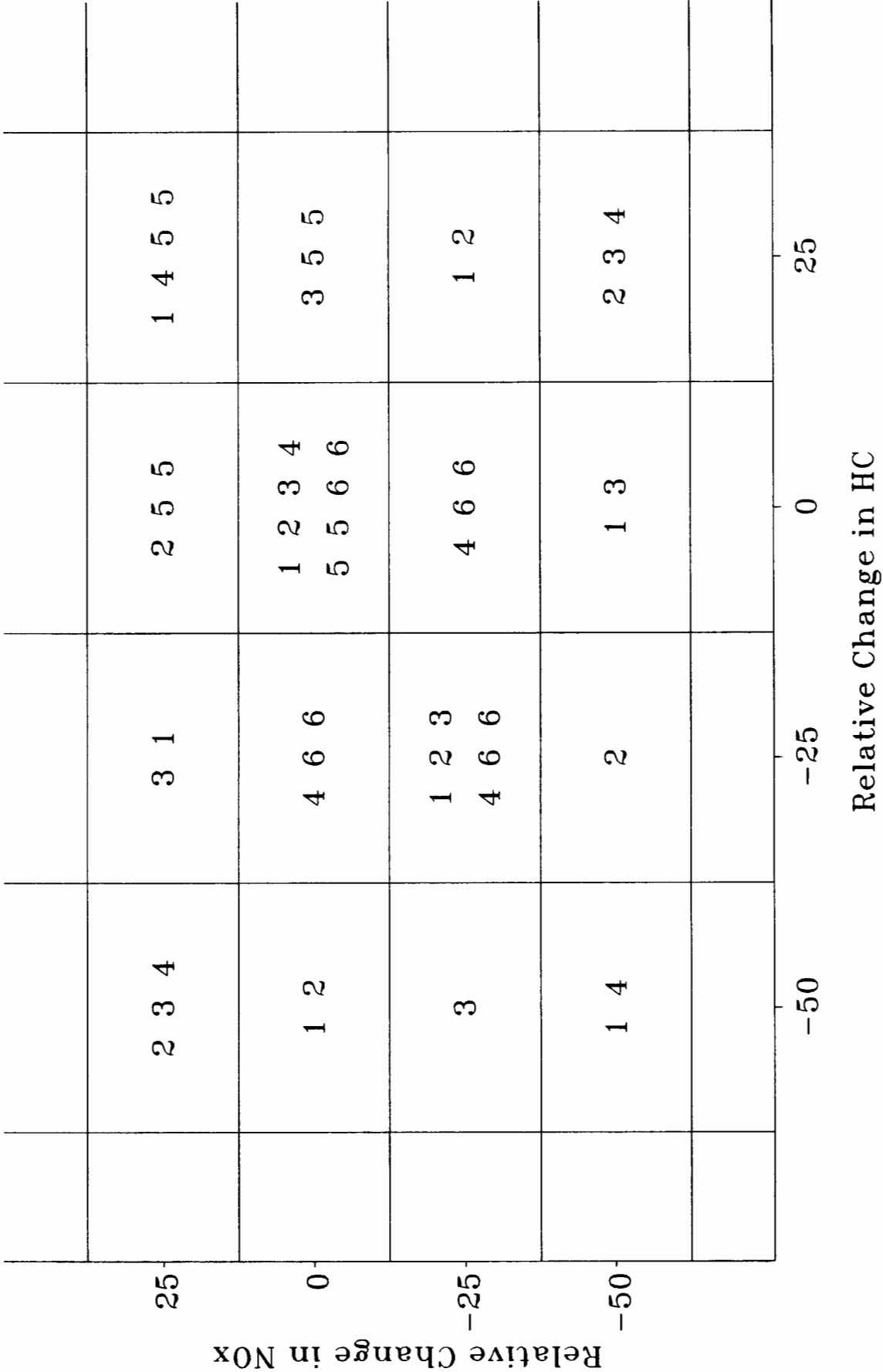
Fig. 4. Distribution of Initial Precursor Combinations Throughout the Experimental Region

= DOWNTOWN LOS ANGELES
= CLAREMONT

NOx (ppb)

HC (ppbC)
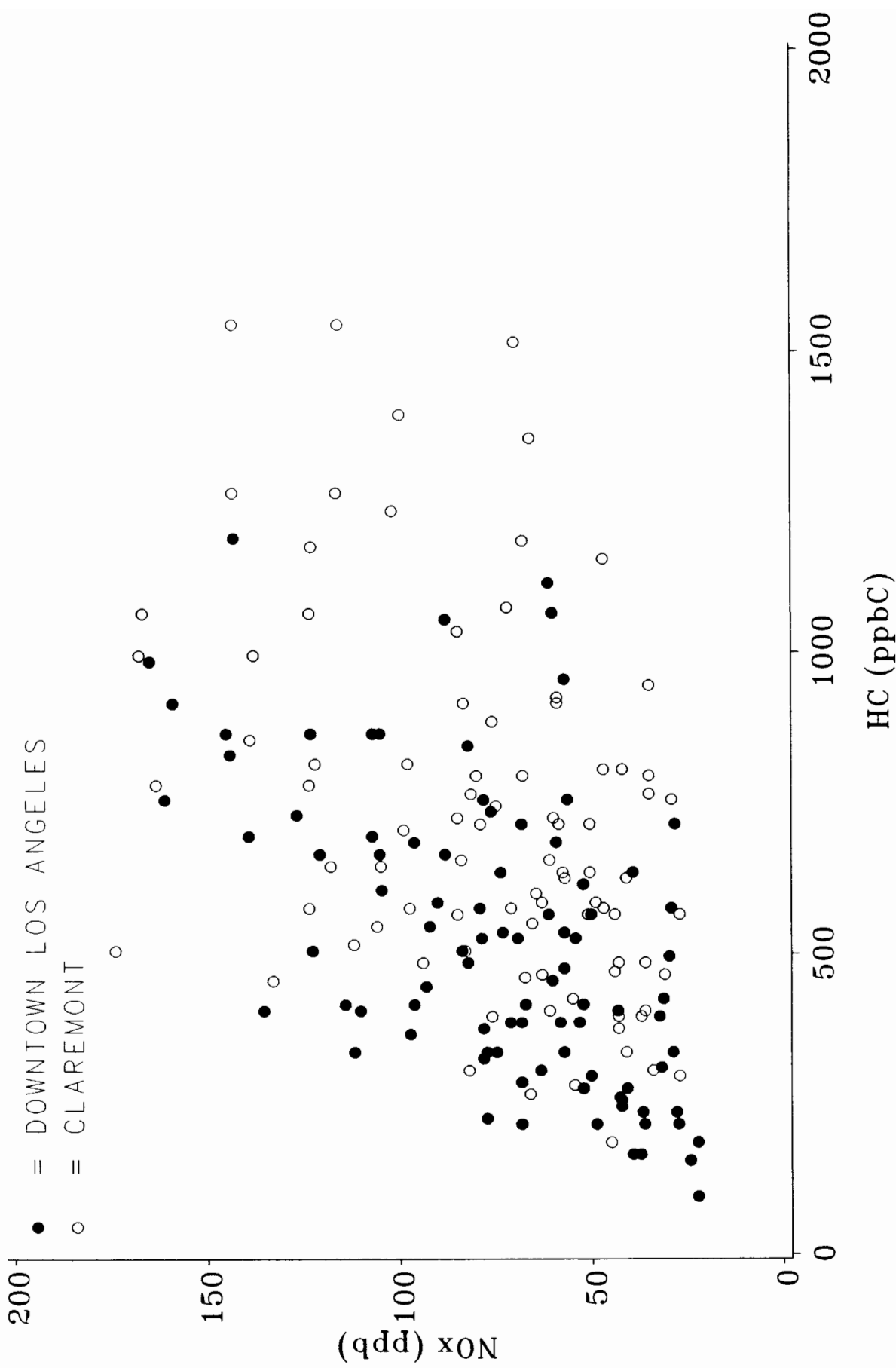
Fig. 5. Box Plots of Day-to-Day Variability in Ozone Differences from Control Bags; (A,B) Denotes RHC = A% and RNOx = B%
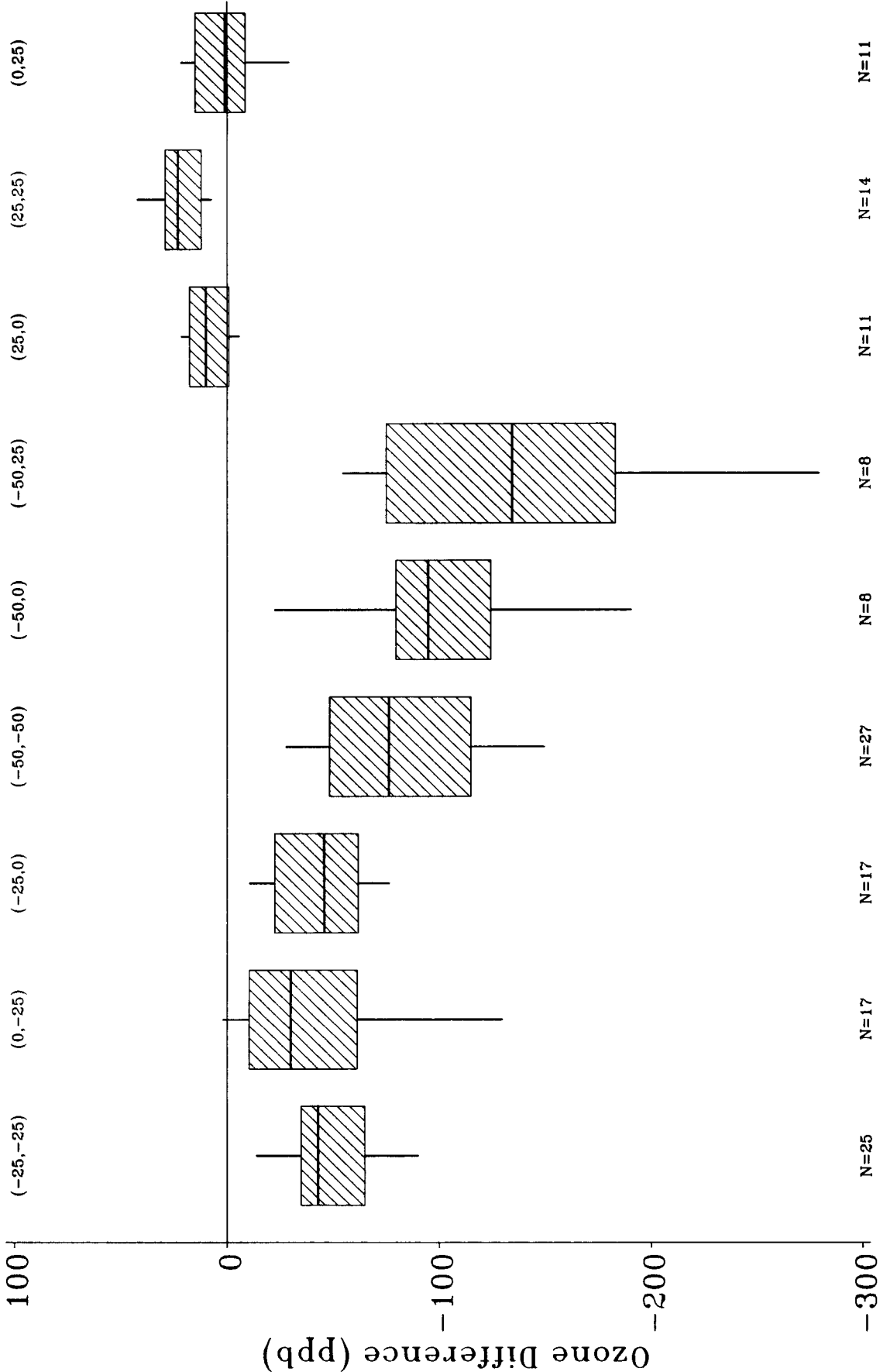
Fig. 6. Fitted Ozone (ppb) Contours: Nonlinear MEM Fit
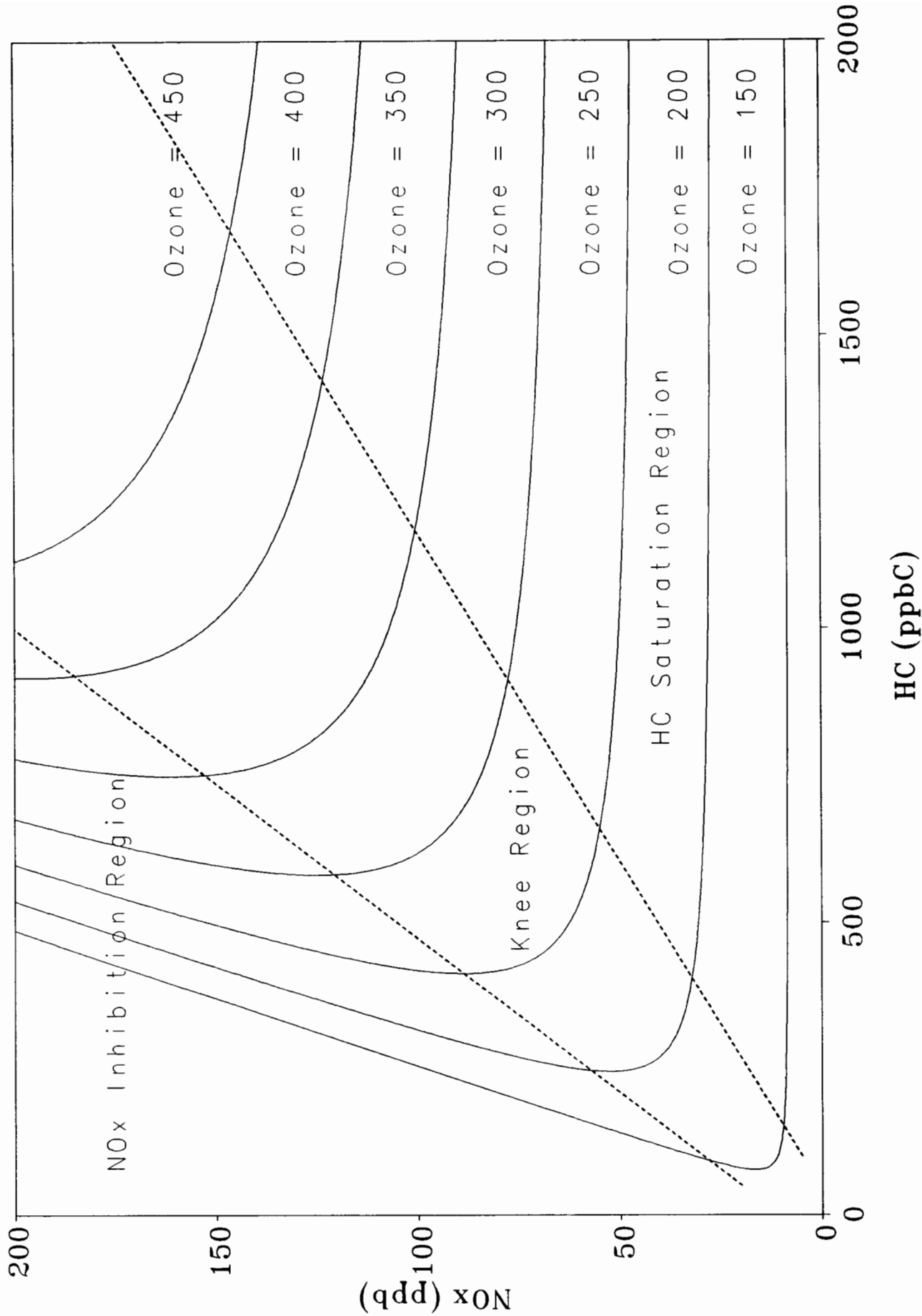
Fig. 7. Fitted Ozone Surface: Nonlinear MEM Fit
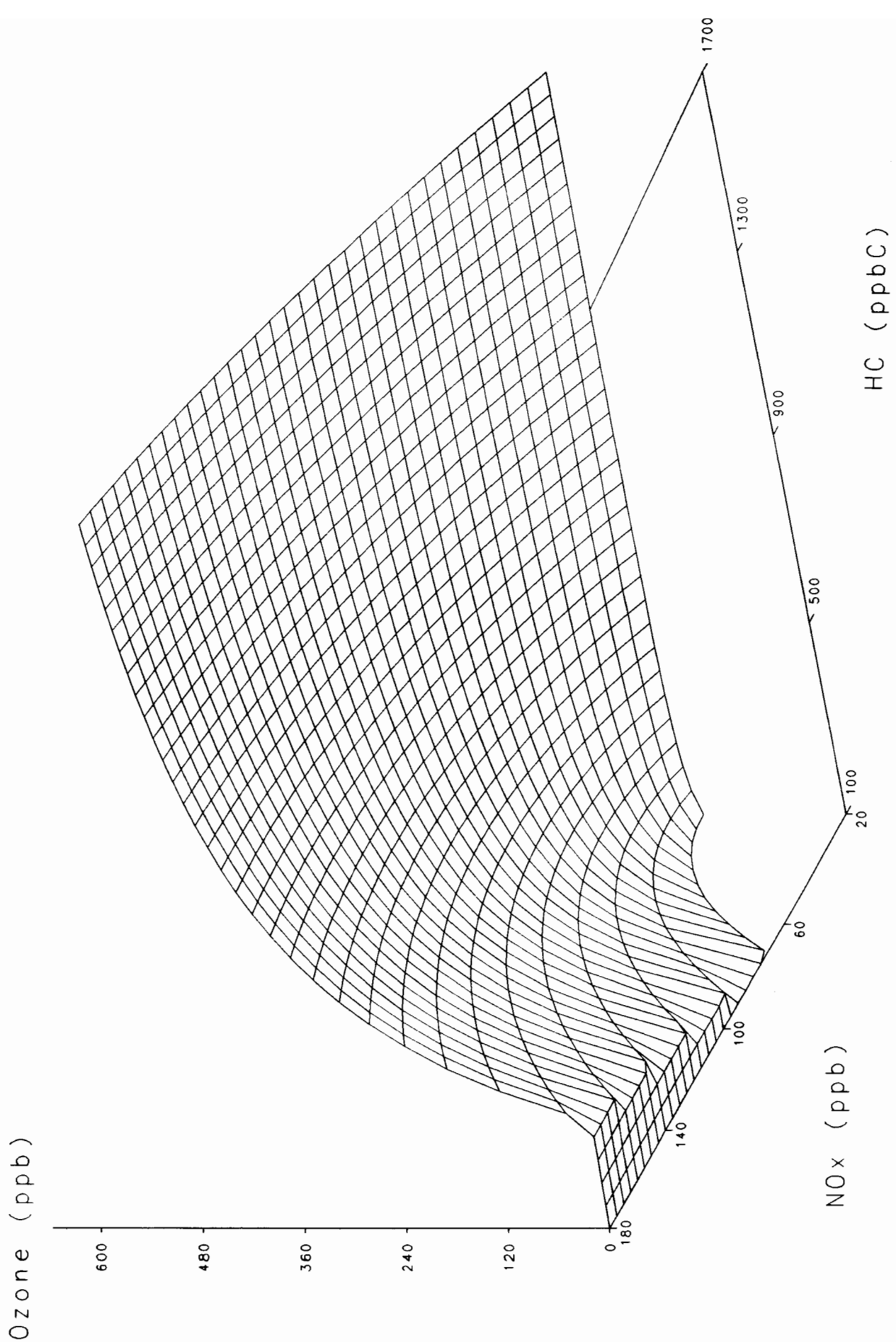
Fig 8. Distribution of HC and NOx Combinations

• = Fractional Factorial
○ = Special Test Runs

NOx (ppb)

HC (ppbC)